



HAL
open science

N-Heterocyclic Carbene Based Tri-organyl-Zn-Alkyl Cations: Synthesis, Structures, and Use in CO₂ Functionalization

David Specklin, Christophe Fliedel, Christophe Gourlaouen, Jean-Charles Bruyere, Teresa Avilés, Corinne Boudon, Laurent Ruhlmann, Samuel Dagorne

► **To cite this version:**

David Specklin, Christophe Fliedel, Christophe Gourlaouen, Jean-Charles Bruyere, Teresa Avilés, et al.. N-Heterocyclic Carbene Based Tri-organyl-Zn-Alkyl Cations: Synthesis, Structures, and Use in CO₂ Functionalization. *Chemistry - A European Journal*, 2017, 23 (23), pp.5509-5519. 10.1002/chem.201605907 . hal-02121106

HAL Id: hal-02121106

<https://hal.science/hal-02121106>

Submitted on 4 Feb 2022

HAL is a multi-disciplinary open access archive for the deposit and dissemination of scientific research documents, whether they are published or not. The documents may come from teaching and research institutions in France or abroad, or from public or private research centers.

L'archive ouverte pluridisciplinaire **HAL**, est destinée au dépôt et à la diffusion de documents scientifiques de niveau recherche, publiés ou non, émanant des établissements d'enseignement et de recherche français ou étrangers, des laboratoires publics ou privés.

NHC-based tri-organyl Zn alkyl cations: synthesis, structure, isomerization for improved stability and use in CO₂ functionalization

David Specklin,^[a] Christophe Fliedel,^[a,b] Christophe Gourlaouen,^[a] Jean-Charles Bruyere,^[a] Teresa Avilés,^[b] Corinne Boudon,^[a] Laurent Ruhlmann,^[a] and Samuel Dagorne^{*[a]}

Dedication ((optional))

Abstract: Tri-organyl and tri-coordinate *N*-heterocyclic carbene Zn–NHC alkyl cations ($(n\text{NHC})_2\text{Zn–Me}^+$ ($n\text{NHC}$ = C2-bonded-IMes-/IDipp; 3^+ and 4^+) were first synthesized and structurally characterized *via* ionization of the corresponding neutral precursors (NHC)ZnMe₂ with [Ph₃C][B(C₆F₅)₄] in the presence of 1 equiv. of free NHC. Cations 3^+ – 5^+ are the first Zn cations of the type Zn(C)(C')(C'')⁺ (C, C', C'' = σ -donor carbyl ligand). While cation $(n\text{IMes})_2\text{Zn–Me}^+$ (3^+) is stable, its sterically congested analogue $(n\text{IDipp})_2\text{Zn–Me}^+$ (4^+) readily undergoes a *n*NHC-to-*a*NHC isomerization in the presence of THF or IDipp to afford the more thermodynamically stable $(a\text{Dipp})(n\text{IDipp})\text{Zn–Me}^+$ ($a\text{Dipp}$ = C5-bonded IDipp, 5^+), reflecting the adaptable-to-sterics coordination chemistry of these cations for improved stability. Kinetic studies combined with DFT calculations agree with a *n*NHC-to-*a*NHC process proceeding through the initial deprotonation of 4^+ (at a Zn-bonded C5-IDipp moiety) by IDipp. Unlike cations $(n\text{NHC})_2\text{Zn–Me}^+$ 3^+ and 4^+ , cation 5^+ reacts with CO₂ through insertion into the Zn-alkyl bond yielding the corresponding Zn(κ^2 -OAc)⁺ cation 6^+ . Both cations 5^+ and 6^+ were successfully used in CO₂ hydrosilylation catalysis for silylformate formation.

Introduction

Zinc–alkyl species have a long-standing tradition as versatile and useful compounds enabling various stoichiometric or catalytic transformations, perhaps most notably as reagents for the reduction of unsaturated polar substrates.^[1] Though much less studied than their neutral analogues ZnR₂, discrete Zn(II) cationic alkyl of the general type [(L)Zn-R]⁺ are of interest for small molecules activation/functionalization due to the enhanced Lewis acidity of the Zn(II) center combined with a nucleophilic Zn–R moiety.^[2] A number of discrete heteroatom-stabilized (primarily *N*-/*O*-/*P*-based ligands) Zn(II) alkyl cations have thus far been structurally characterized.^[3] Recently, the use of weakly

coordinating and inert anions such as the carborane anion CHB₁₁Cl₁₁[−] and the aluminate anion Al{OCH(CF₃)₂}₄[−] allowed the isolation and structural characterization of salt species, such as [Et-Zn(η^3 -toluene)][CHB₁₁Cl₁₁][−] and Et-Zn[Al{OCH(CF₃)₂}₄][−], both containing a weakly bonded and thus quite reactive “Zn–Et⁺” entity.^[4] Dinuclear triple-decker Zn cations of the type Cp⁺₃Zn₂⁺ are also known.^[5] Despite their attractive features, including a cheap and non-toxic metal source, the use of cationic Zn(II) electrophilics for small molecules activation and catalysis remains quite limited, which may perhaps be related to the limited hydrolytic stability of such electrophilic organometallics. Thus far, well-defined Zn(II) cationic alkyls have been shown to be efficient catalysts/precatalysts for alkene/alkyne hydroamination reactions as well as ring-opening polymerization of cyclic ethers/esters.^[3,4,5a,6] A recent report also mentioned that strong Lewis acid [Et-Zn(η^3 -toluene)(κ^2 -CHB₁₁Cl₁₁)] may catalytically hydrosilylate CO₂ to CH₄, presumably *via* a Lewis-acid-activation mechanism.^[7]

Due to their strong σ -donating properties and steric tunability, *N*-heterocyclic carbenes (NHCs) are exceptional ligands for the stabilization of various metal/heteroatom centers, including oxophilic and electron-poor metal centers such as Zn(II).^[8,9] The use of neutral and robust NHC–Zn adducts for effective zinc-mediated catalytic processes is currently attracting interest, and includes the recent development of Zn–NHC catalysts in imine hydrogenation, CO₂ reductive amination, allylic alkylation and cyclic esters/carbonates polymerization.^[10,11] Two examples of NHC-stabilized Zn(II) hydride cations were also reported to catalyze ketone or/and CO₂ hydrosilylation.^[12]

We are interested in NHC-stabilized Zn alkyl cations of the type (NHC)₂Zn–R⁺ as potentially robust, yet electrophilic, Zn-based organometallics for subsequent small molecules activation and use in catalysis. Besides potential enhanced stability, such targets are structurally interesting as unprecedented Zn cations of the type [Zn(C)(C')(C'')]⁺ (C, C', C'' = σ -donor carbyl ligand).^[13] Our earlier studies on mono-NHC Zn(II) cations (NHC)Zn(Me)(THF)_x⁺ (x = 1, 2) concluded on their limited stability under polymerization catalysis conditions,^[11] prompting us towards (NHC)₂Zn–R⁺ cations, expected to be more robust.

Herein we first report on the synthesis, structure and reactivity with CO₂ of three-coordinate tris-organyl (NHC)₂Zn–Me⁺ cations. In addition to structural aspects, including an unexpected *n*NHC-to-*a*NHC rearrangement (*n*NHC, *a*NHC = C2- and C5-bonded NHC, respectively),^[14] the ability of such cations to stoichiometrically and catalytically functionalize CO₂ is also

[a] Dr. D. Specklin, Dr. C. Fliedel, Dr. C. Gourlaouen, J.-C. Bruyere, Prof. C. Boudon, Prof. L. Ruhlmann, Dr. S. Dagorne
Institut de Chimie de Strasbourg, CNRS
Université de Strasbourg
1, rue Blaise Pascal, 67000 Strasbourg (France)
E-mail: dagorne@unistra.fr

[b] Dr. C. Fliedel, Prof. T. Avilés
LAQV, REQUIMTE, Departamento de Química
Faculdade de Ciências e Tecnologia
Universidade Nova de Lisboa, 2829-516 Caparica (Portugal)

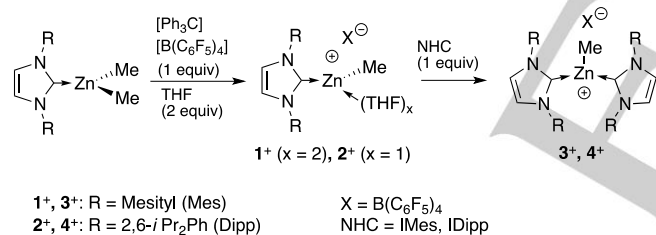
Supporting information for this article is given via a link at the end of the document. ((Please delete this text if not appropriate))

discussed. All experimental studies are complemented/supported by DFT calculations when appropriate.

Results and Discussion

Synthesis and Structure of tris-carbyl Zn(II) (NHC)₂Zn-Me⁺ cations **3**⁺, **4**⁺ and **5**⁺.

Tris-carbyl Zn cations (*n*IMes)₂ZnMe⁺ [**3**⁺, *n*IMes = 1,3-bis-(2,4,6-trimethylphenyl)imidazolin-2-ylidene] and (*n*IDipp)₂ZnMe⁺ [**4**⁺, *n*IDipp = 1,3-bis-(2,6-diisopropylphenyl)imidazolin-2-ylidene] were prepared *via* ionization of neutral precursors (NHC)ZnMe₂ with [Ph₃C][B(C₆F₅)₄] and subsequent addition of a second NHC ligand (Scheme 1). The mono-NHC and THF-stabilized Zn-Me⁺ (*n*IMes)Zn(Me)(THF)₂⁺ (**1**⁺) and (*n*IDipp)Zn(Me)(THF)⁺ (**2**⁺) were first generated *in situ* *via* a Me⁻ abstraction reaction between an equimolar amount of (NHC)ZnMe₂ and [Ph₃C][B(C₆F₅)₄] in the presence of THF (Scheme 1). Subsequent addition with 1 equiv. of *n*IMes and *n*IDipp led to the quantitative formation of tris-organyl Zn-Me cations **3**⁺ and **4**⁺, respectively, as B(C₆F₅)₄⁻ salts with no apparent cation/anion interactions in solution on the basis of multinuclear NMR data. The ¹³C NMR singlet resonance for the Zn-C_{NHC} carbon (δ = 177.0 and 178.9 ppm for **3**⁺ and **4**⁺, respectively) is significantly upfield relative to that in (IMes)ZnMe₂ and (IDipp)ZnMe₂ (δ = 189.7 and 188.6 ppm, respectively), consistent with a more Lewis acidic Zn(II) center in **3**⁺ and **4**⁺.^[15]



Scheme 1. Synthesis of the tris-organyl Zn alkyl cations **3**⁺ and **4**⁺.

Salts [**3-4**][B(C₆F₅)₄] were isolated in good yield (82% and 78% yield, respectively) as analytically pure colorless solids, but display a different stability. Remarkably, salt [**3**][B(C₆F₅)₄] is air-stable in the solid state and for days in CD₂Cl₂ (under N₂), indicating the effective steric and electronic stabilization of the Zn-Me⁺ moiety by two NHCs in cation **3**⁺. In contrast, [**4**][B(C₆F₅)₄] decomposes within minutes under air and is unstable in CD₂Cl₂ (room temperature). The severe steric hindrance in cation **4**⁺ (*vide infra* for its solid state structure) explains its limited hydrolytic stability. Salt [**4**][B(C₆F₅)₄] is however stable for days at room temperature in C₆D₅Br.

The molecular structures of salts [**3-4**][B(C₆F₅)₄] were confirmed by X-ray crystallographic analysis (Figures 1 and 2; Table S1, Supporting Information), establishing **3**⁺ and **4**⁺ as tri-organyl, three-coordinate (NHC)₂ZnMe⁺ cations. In **3**⁺, the Zn center lies in a slightly distorted trigonal geometry environment

[C_{NHC}-Zn-C_{NHC} = 126.5(2)°]. Due to the cationic charge on Zn(II), the Zn-C_{NHC} bond distances [2.059(6) and 2.044(6) Å] are shorter than in (IDipp)ZnMe₂ [2.112(2) Å].^[11] The angles between the NHC (rings) average planes and the nearly planar ZnC₃ array (65.1° in average) are such that they minimize steric interactions between the four mesityl substituents, the latter providing a significant protection to the metal center. In contrast, the coordination of two *n*IDipp ligands to Zn(II) in cation **4**⁺ results in severe steric congestion, as reflected by a much larger C_{NHC}-Zn-C_{NHC} angle [135.67(8)°] than in **3**⁺ [126.5(2)°] (Figures 1 and 2). Also, the larger “pitch” angles (*i.e.* angle between a given Zn-C_{NHC} bond and the associated NHC ring) in **4**⁺ vs. **3**⁺ [26.8(2)° average vs. 13.2(4) and 9.2(4)°] are indicative of severe steric crowding in **4**⁺.

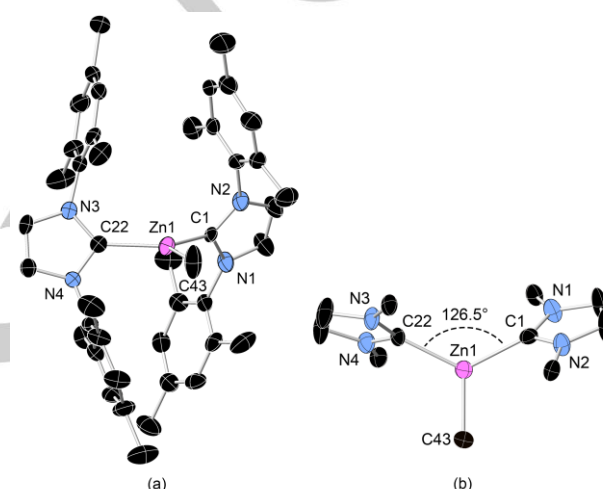


Figure 1. Molecular structure of cation (*n*IMes)₂ZnMe⁺ (**3**⁺). (a) front view; (b) ZnC₃ coordination plane in **3**⁺ with selected atoms only. Selected bond lengths (Å) and angles (°): Zn(1)-C(1) = 2.059(6), Zn(1)-C(22) = 2.044(6), Zn(1)-C(43) = 1.960(6), C(22)-Zn(1)-C(1) = 126.5(2), C(22)-Zn(1)-C(43) = 117.2(3), C(1)-Zn(1)-C(43) = 116.2(3).

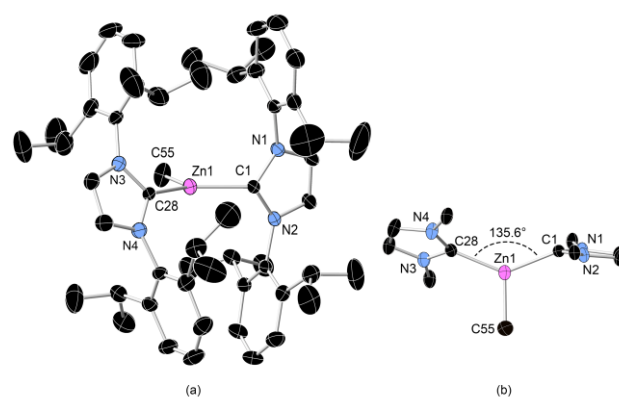
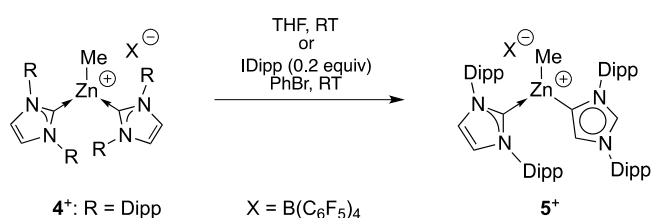


Figure 2. Molecular structure of cation (*n*IDipp)₂ZnMe⁺ (**4**⁺). (a) front view; (b) ZnC₃ coordination plane in **4**⁺ with selected atoms only. Selected bond lengths (Å) and angles (°): Zn(1)-C(1) = 2.077(2), Zn(1)-C(28) = 2.068(2), Zn(1)-C(55) = 1.983(3), C(28)-Zn(1)-C(1) = 135.67(8), C(28)-Zn(1)-C(55) = 113.3(1), C(1)-Zn(1)-C(55) = 111.0(1).

Normal-to-abnormal NHC rearrangement in $(\text{NHC})_2\text{Zn-Me}^+$ cations: access to cation $(\text{IDipp})(\text{aIDipp})\text{Zn-Me}^+$ (5^+ , $\text{aIDipp} = \text{C4/C5-bonded IDipp}$).

Though stable for days in PhBr, cation 4^+ is unstable in a coordinative solvent such as THF to slowly and quantitatively isomerize (48h, room temperature) to cation $(\text{IDipp})(\text{aIDipp})\text{Zn-Me}^+$ (5^+ ; Scheme 2), as deduced from NMR data. The formation of cation 5^+ thus arises from a normal-to-abnormal NHC rearrangement of one IDipp ligand in 4^+ , a reaction apparently promoted by THF and driven by steric relief as deduced from experimental/DFT studies (*vide infra*). A few examples of well-identified *n*NHC-to-*a*NHC isomerization are known for Fe(II), Y(III) and group 13 element NHC adducts.^[16]



Scheme 2. *n*NHC-to-*a*NHC isomerization of cation 4^+ to its isomer 5^+ .

In contrast, the less sterically bulky cation 3^+ showed no sign of decomposition in refluxing THF (thf-*d*⁶, 24 h, 80 °C). The conversion of 4^+ to 5^+ may also be thermally promoted though it proceeds sluggishly: heating a PhBr solution of cation 4^+ (90 °C, 3 h) led to the complete consumption of 4^+ and the formation of cation 5^+ (only 50% conversion to 5^+ ; C_6Me_6 was used as an internal standard) along with unidentified species. Salt $[\mathbf{5}][\text{B}(\text{C}_6\text{F}_5)_4]$ was isolated in a pure form (77% yield) as a colorless and air-stable solid, contrasting with the poor hydrolytic stability of its parent compound $[\mathbf{4}][\text{B}(\text{C}_6\text{F}_5)_4]$.

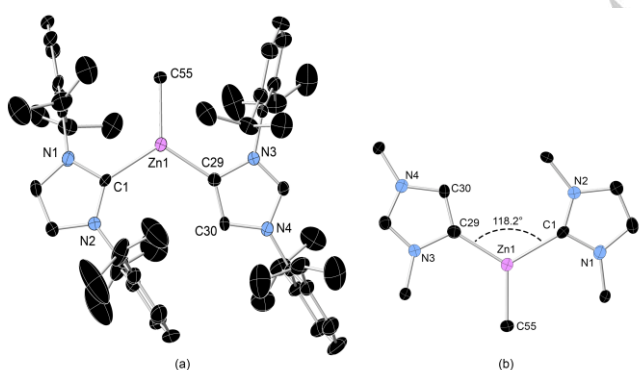


Figure 3. Molecular structure of cation $(\text{nIDipp})(\text{aIDipp})\text{ZnMe}^+$ (5^+). (a) Front view; (b) ZnC_3 coordination plane in 5^+ with selected atoms only. Selected bond lengths (Å) and angles (°): $\text{Zn}(1)\text{-C}(1) = 2.098(2)$, $\text{Zn}(1)\text{-C}(29) = 2.029(3)$, $\text{Zn}(1)\text{-C}(55) = 1.997(4)$, $\text{C}(29)\text{-Zn}(1)\text{-C}(1) = 118.2(2)$, $\text{C}(29)\text{-Zn}(1)\text{-C}(55) = 121.7(2)$, $\text{C}(1)\text{-Zn}(1)\text{-C}(55) = 120.1(2)$.

As confirmed by X-ray crystallography, the molecular structure of cation 5^+ thus displays a central tri-coordinate $\text{Zn}(\text{II})\text{-Me}$ cation stabilized by a *n*IDipp and an *a*IDipp ligand, allowing a significant steric decompression when compared to cation 4^+ . This is best reflected by a nearly co-planar arrangement of the " $(\text{nNHC})(\text{aNHC})\text{Zn-Me}$ " moiety with an average angle of $8.0(1)^\circ$ between the NHC rings (average plane) and the ZnC_3 planar array (vs. 65.1° in parent cation 4^+ , *vide supra*). Furthermore, unlike cation 4^+ , the Zn-NHC bonds in cation 5^+ display little geometrical distortions (Zn-NHC "pitch" angles of $1.2(1)^\circ$ in 5^+ vs. $26.8(2)^\circ$ average in 4^+). The Zn- C_{aNHC} bond distance [$2.029(3)$ Å] is similar to that in known *a*NHC-Zn complexes.^[17]

To gain further insight on the relative stability of cations $(\text{NHC})_2\text{Zn-Me}^+$, DFT calculations were performed (at the BLYP/def2-SVP level, Figure 4; Figure S27, Supporting Information). In line with experimental results, model cation $(\text{nIDipp})_2\text{Zn-Me}^+$ (IV) is less stable by 6.6 kcal/mol than isomer $(\text{nIDipp})(\text{aIDipp})\text{Zn-Me}^+$ (V). On the contrary, the less sterically congested model cation $(\text{nIMes})_2\text{Zn-Me}^+$ (III) was computed to be more stable (by 7.3 kcal/mol) than isomer $(\text{nIMes})(\text{aIMes})\text{Zn-Me}^+$ (III'), not observed experimentally, thus indicating the electronic preference for *n*NHC vs. *a*NHC ligation in NHC-Zn(II) cationic systems. The better thermodynamic stability of model V over IV thus arises from severe steric congestion in IV .^[18]

NBO analysis provided further information on the bonding of IV and V (Tables S2 and S3, ESI). In IV , the Wiberg indexes (WI) for the Zn- C_{NHC} (0.28) and Zn-alkyl (0.40) bonds agree with a covalent bonding with a strong ionic component, as expected with a cationic Zn(II) center. Due the partial vinylic character of the *a*NHC ligand, the C_{aNHC} partial charge (-0.39) is larger than for the C_{nNHC} atoms in IV and V (-0.07 average). The partial charge at Zn(II) is essentially unchanged upon going from IV to V (1.40 and 1.38, respectively), suggesting little electronic effect at the metal center upon *n*NHC-to-*a*NHC isomerization and thus indicating a more polar Zn-*a*NHC vs. Zn-*n*NHC bond in V .

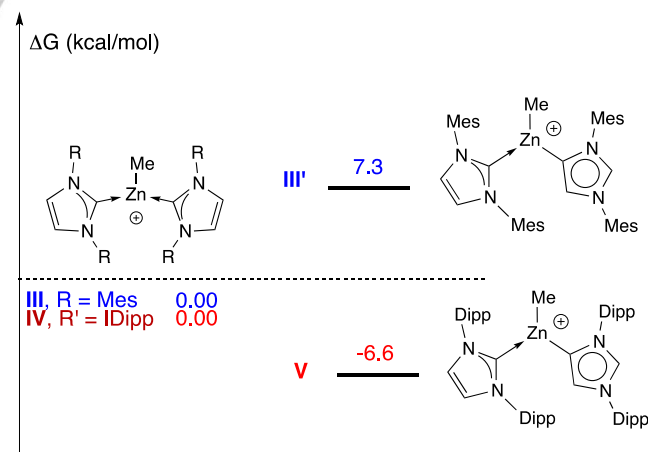


Figure 4. DFT-calculated Gibbs free energy (BLYP/def2-SVP, gas phase) for the $(\text{NHC})_2\text{ZnMe}^+$ models III , III' , IV and V .

*n*NHC-to-*a*NHC isomerization mechanism of (NHC)₂ZnMe⁺ cations: kinetic and DFT studies.

Reports on *n*NHC-to-*a*NHC isomerization in NHC metal complexes suggest a mechanism greatly dependent on the nature of the NHC ligand and the metal center.^[16g-i] The isomerization mechanism of cation **4**⁺ to **5**⁺ was thoroughly investigated. As noted above, cation **4**⁺ is stable for days in PhBr but slowly converts to **5**⁺ in the presence of THF, suggesting an initial THF-promoted NHC decooordination (from cation **4**⁺) to afford free IDipp that may then promote the isomerization reaction. Monitoring (by ¹H NMR) the conversion of **4**⁺ to **5**⁺ (thf-d₆, 48 h, room temperature) showed no evidence of NHC dissociation (and no trace of free NHC) as the isomerization proceeds. However, the NMR scale reaction of **4**⁺ with IDipp (0.2 equiv., C₆D₅Br, room temperature, 60 h) led to the quantitative formation of cation **5**⁺ (along with 0.2 equiv. of NHC), thus suggesting an IDipp-catalyzed isomerization. No intermediate species were observed prior to formation of the final product **5**⁺.

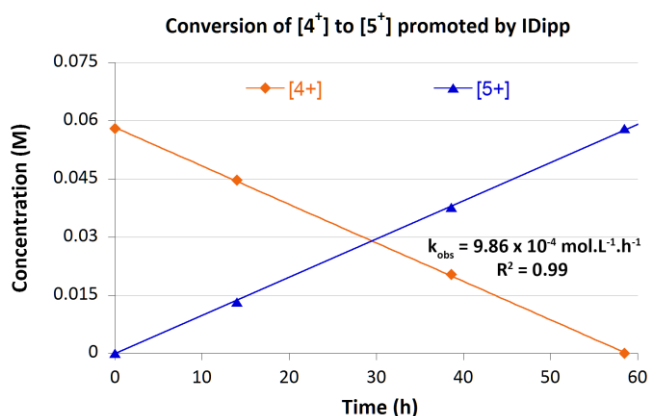


Figure 5. Conversion plot of formation/consumption of cation **4**⁺/**5**⁺ versus time ([**4**⁺]₀ = 0.06 M, 0.2 equiv. of IDipp, C₆D₅Br, room temperature).

To better understand the *n*NHC-to-*a*NHC isomerization process, kinetic studies of the conversion of **4**⁺ to **5**⁺ were performed in the presence of IDipp ([**4**⁺]₀ = 0.06 M, 0.2 equiv. of IDipp, C₆D₅Br, room temperature). As depicted in Figure 5, the consumption/formation rate of cation **4**⁺/**5**⁺ follows a pseudo-zero order rate law ($k_{\text{obs}} = 9.86 \times 10^{-4} \text{ mol.l}^{-1}.\text{h}^{-1}$) till complete conversion to **5**⁺ (Figure S10, Supporting Information). The rate dependence on cation **4**⁺ and IDipp was also estimated using the initial reaction rates method (Figure 6; Figures S11-S19, Supporting Information). The reaction rate was found to be first order relative to IDipp while, somewhat unexpectedly, an inverse first order dependence on **4**⁺ was observed. Thus, increasing the concentration of the starting cation **4**⁺ decreases the rate of its isomerization.

Since the isomerization of **4**⁺ to **5**⁺ necessarily involves a C5-H cleavage of a IDipp moiety, a possible kinetic isotope effect on the reaction rate was studied by monitoring the reaction of C4- and C5-deuterated (IDipp-d₂)₂ZnMe⁺ cation,

prepared using deuterated IDipp (IDipp-d₂) as a NHC source, with 0.2 equiv. of IDipp-d₂ ([**4**-d₂⁺]₀ = 0.06 M, 0.2 equiv. of IDipp-d₂, C₆D₅Br, room temperature).^[19] A nearly identical reaction rate ($k_{\text{obs}} = 1.0 \times 10^{-3} \text{ mol.l}^{-1}.\text{h}^{-1}$) was observed, indicating no isotope effect ($k_{\text{D}}/k_{\text{H}} = 1.02$). This suggests a fast or/and reversible C-H activation, hinting at a reversible deprotonation/protonation process as deduced from DFT studies and discussed below. The quantitative formation of (*n*IDipp-d₂)(*a*IDipp-d₂)Zn-Me⁺ (**5**-d₄⁺) also rules out the involvement of any external proton source for the formation of **5**⁺ (Scheme 3).

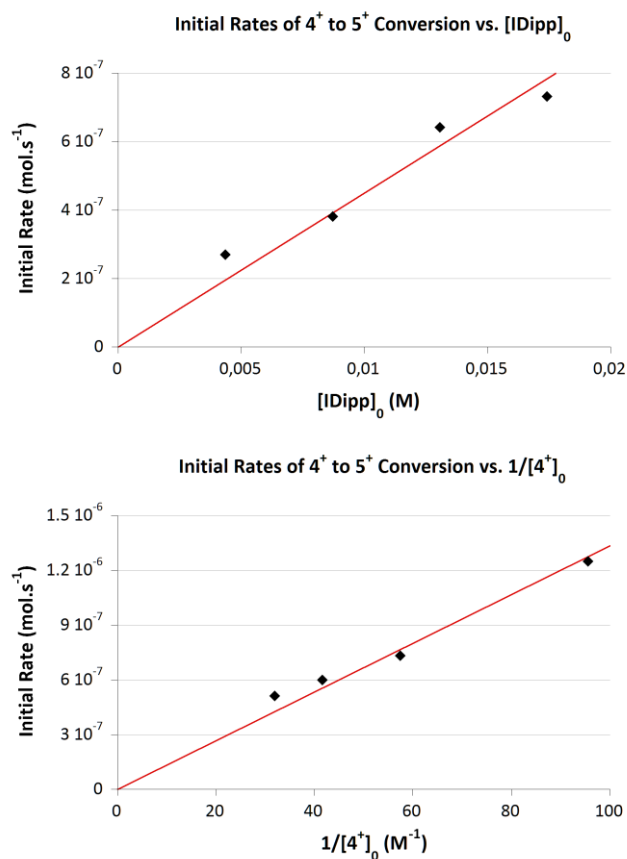
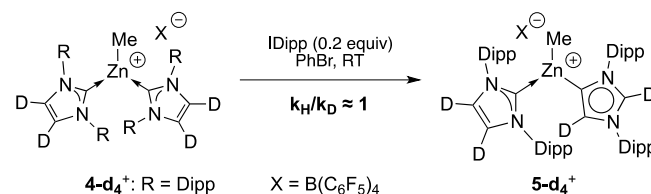


Figure 6. Initial reaction rate dependence on [IDipp]₀ (top, [**4**⁺]₀ = 0.0174 M) and 1/[**4**⁺]₀ (bottom, [IDipp]₀ = 0.0174 M) in the isomerization of **4**⁺ to **5**⁺.



Scheme 3. Isomerization of cation **4**-d₄⁺ to **5**-d₄⁺.

In combination with kinetic data, DFT computation revealed decisive to establish the mechanism of formation of **5**⁺ from **4**⁺ in

the presence of IDipp (Scheme 4 and Figure 7; Figures S28-S33, Supporting Information). First, DFT-modeling the interaction of cation $(n\text{IDipp})_2\text{Zn-Me}^+$ (**IV**) with free IDipp (**Carb**) led to the exergonic formation of cation **A** ($\Delta G = -14.3$ kcal/mol, Figure 7), which features a $\text{C-H}\cdots\text{C}$ hydrogen-bond interaction between IDipp (C2) and one IDipp ligand in cation **IV**. Though **IV** and IDipp do not apparently interact in solution ($^1\text{H NMR}$, $\text{C}_6\text{D}_5\text{Br}$, room temperature), NHCs are well-known strong H-bond acceptors owing to their Brønsted basicity and the acidic character of NHC-C4/C5-H hydrogens is also exemplified.^[20,21] Besides H-bonding, dispersive interactions in **A** (between the incoming IDipp ligand and **IV**) certainly favor its stabilization, as deduced from computed non-covalent interactions for **A** (Figure S28', Supporting Information). H-bonded IDipp in cation **A** is ideally disposed for deprotonation of a C5-H proton, which occurs *via* transition state **TS1** ($\Delta\Delta G = 14.0$ kcal/mol) to afford model **B** ($\Delta G = -0.5$ kcal/mol). The latter can be described as a $(n\text{IDipp})(n\text{IDipp})\text{ZnMe}$ zwitterion stabilized by an IDipp-H^+ cation through strong $\text{C-H}\cdots\text{C}$ interactions. Structurally, the $\text{C-H}\cdots\text{C}$ interaction in model **B** can be related to the experimentally

characterized $(\text{IMes})\text{-H}(\text{IMes})^+$ cation, in which the central proton is coordinated by two NHCs.^[21a] As documented in a few instances, strong bases may deprotonate NHC moieties at C5-H, further substantiating the proposed formation of **B** from **A**.^[22]

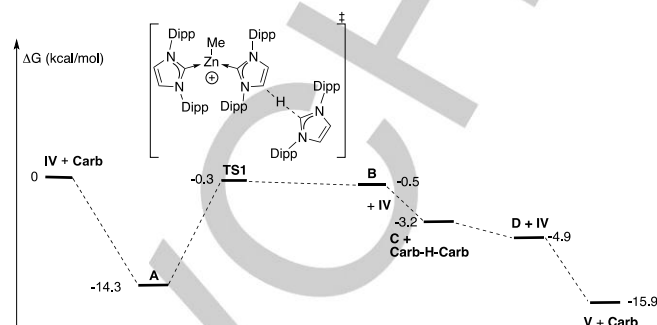
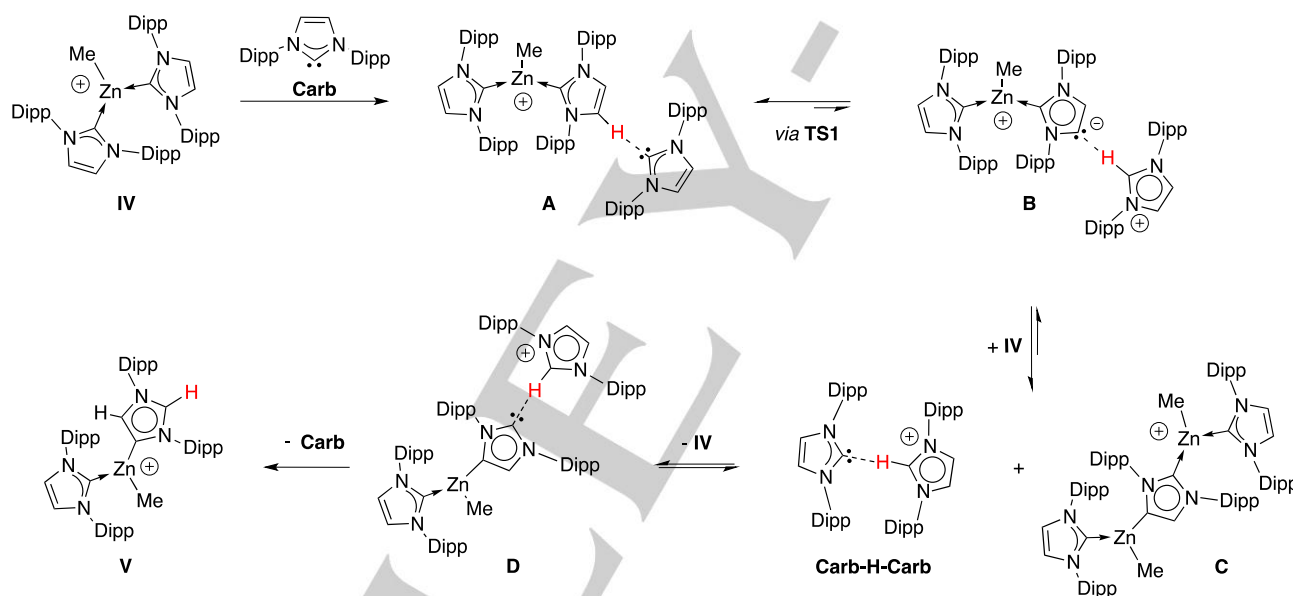


Figure 7. DFT-estimated (BLYP/def2-SVP, gas phase) Gibbs free energy (in kcal/mol) profile for the NHC-catalyzed conversion of **IV** to **V**.



Scheme 4. Proposed mechanism for the NHC-catalyzed isomerization of model cation **IV** to **V**.

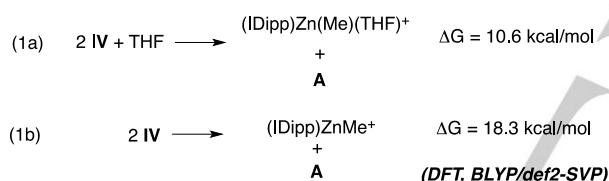
The low energy barrier converting **A** to **B** (14.0 kcal/mol) allows a reaction under thermodynamic control under the studied conditions (room temperature). The higher stability of **A** vs. **B** (by 13.8 kcal/mol) indicates **B** as a minor component. Yet, the formation of **B**, even as a fleeting intermediate, appears crucial for the isomerization reaction to proceed. From **B**, three additional steps were computed as thermodynamically favored with the final formation of **V**. Model **B** may react with cation **IV**, *via* a C5- α NHC nucleophilic attack of **IV**, to produce dinuclear species **C** along with cation $(\text{IDipp})\text{-H}(\text{IDipp})^+$ (**Carb-H-Carb**) with a slightly exergonic reaction ($\Delta\Delta G = -2.7$ kcal/mol). A few examples of dinuclear Zn-NHC species similar to **C** were recently characterized, giving some ground to its viability.^[17a,23]

The IDipp moiety in **Carb-H-Carb** may then undergo a ligand substitution at **C** yielding mononuclear species **D** and regenerating $(\text{IDipp})_2\text{ZnMe}^+$ (**IV**), a reaction slightly favored ($\Delta\Delta G = -1.7$ kcal/mol). An intramolecular proton transfer in **D** then affords the final and most thermodynamically stable product $(n\text{IDipp})(n\text{IDipp})\text{ZnMe}$ (**V**, $\Delta\Delta G = -11$ kcal/mol). The last step also regenerates free carbene IDipp, which thus acts as catalyst as experimentally observed. Overall, the DFT-estimated mechanism of the IDipp-catalyzed conversion of **IV** to **V** is under thermodynamic control and proceeds *via* an initial **A/B** equilibrium that readily occurs upon combining cation **IV** with **Carb**. Though **B** is a minor component, its continuous and irreversible conversion to most stable **V** (through intermediates

C and **D**) displaces the **A/B** equilibrium till complete consumption of **A** (and thus **IV**). The comparable thermodynamic stabilities of intermediates **B**, **C** and **D** allow such species to equilibrate as the reaction proceeds.

Though the rate-determining step of the **IV**-to-**V** isomerization may not be inferred from the available experimental and computational data, the present mechanism allows a rationale of the kinetic data. Assuming an equilibrium of **C** and **Carb-H-Carb** with **D** and **IV** (Scheme 4), increasing the concentration of **IV** will disfavor the formation of **D**, the key intermediate that irreversibly yields final product **V**, thereby decreasing the reaction rate. This explains the observed inverse order dependence of the reaction rate on **4**⁺. Also, the observed pseudo-zero-order reaction rate (for the consumption/formation of cation **4**⁺/**5**⁺) is also compatible with the proposed mechanism: *i.e.* the involvement of a minor intermediate (*i.e.* **B**), formed immediately upon combining **IV** and **Carb** and continuously replenished from a larger pool (*i.e.* **A**) till complete consumption of **A** (and thus **IV**).

The THF-promoted isomerization of **4**⁺ to **5**⁺ may also be understood in light of the above, assuming THF substitution of a NHC ligand (at **IV**) occurs to some extent. As shown in eq. 1a, the formation of cation (IDipp)Zn(Me)(THF)⁺ and **A** (from THF and **IV**) is only endergonic by 10.6 kcal/mol. In the absence of THF, the formation of **A** is disfavored by 18.3 kcal/mol (eq. 1b).



Note that the present mechanism differs from that in neutral NHC–Al(III) species, for which an initial and quantitative NHC decoordination from the *n*NHC–metal adduct was observed. A fast *n*NHC/*a*NHC equilibrium was proposed to explain the formation of the *a*NHC–Al(III) species.^[169] For the present Zn cations, such a mechanism is clearly ruled out on the basis of kinetic data.

Reactivity of (NHC)₂ZnMe⁺ cations with CO₂: insertion chemistry and derived hydrosilylation catalysis.

Metal-based CO₂ functionalization catalysis is currently attracting significant attention to access valuable CO₂-based small molecules such as formate- and methanol-equivalent derivatives, typically through CO₂ hydrogenation and hetero-elementation (primarily hydrosilylation and hydroboration).^[24,25] Given the low cost and toxicity of Zinc, Zn-based species for CO₂ functionalization catalysis are emerging and include, most notably, a few examples of ligand-supported Zn(II) hydride catalysts for CO₂ hydrosilylation with a catalysis proceeding with an initial CO₂ insertion into the Zn–H bond.^[12,25-27] Despite their better availability and thermal/hydrolytic stability (*vs.* Zn–hydride analogues), Zn–alkyl species have been little studied for CO₂ functionalization,^[7,28] perhaps owing to the long-known inertness of zinc dialkyls towards CO₂, frequently attributed to the

moderate nucleophilicity/Lewis acidity of the Zn–R group/Zn(II) center in such compounds.^[29] The carboxylation of Zn–R species may be metal-catalyzed,^[30] but direct (and uncatalyzed) CO₂ insertion of discrete Zn–alkyl species is not documented.^[31] The reactivity of Lewis acidic (NHC)₂ZnMe⁺ **3-5**⁺ with CO₂ was thus studied, which led to further developments in hydrosilylation catalysis.

Cations (*n*NHC)₂ZnMe⁺ (**3**⁺-**4**⁺) immediately reacted with CO₂ (1.5 atm. CO₂, C₆D₅Br, room temperature, 15 min.) yet to afford a complicated mixture of species, out of which only the corresponding NHC–CO₂ zwitterionic adducts could be identified by ¹H and ¹³C NMR (Scheme 5).^[32] For the CO₂ reaction with **3**⁺, the IMes–CO₂ adduct was isolated (47% yield) and its molecular structure confirmed by X-ray crystallography (Figure S9, Supporting Information). The formation of NHC–CO₂ adducts suggests a preferred CO₂ insertion into the Zn–C_{NHC} (*vs.* the Zn–Me) bond of **3**⁺ and **4**⁺.^[33] In contrast, a selective CO₂ insertion in the Zn–Me bond is observed upon reaction of (*n*IDipp)(*a*IDipp)ZnMe⁺ (**5**⁺) with CO₂ (1.5 atm., C₆D₅Br, room temperature, 12 h) with the quantitative formation of the Zn–OAc cation (*n*IDipp)(*a*IDipp)Zn(κ²-OAc)⁺ (**6**⁺, Scheme 5), indicating that “(*n*NHC)(*a*NHC)” coordination provides a superior ancillary to the Zn–Me⁺ moiety in the present systems.

The formation of cation **6**⁺ from **5**⁺ and CO₂ is the first instance of direct CO₂ insertion into a well-defined Zn–alkyl species. Salt [**6**][B(C₆F₅)₄] was isolated as a colorless solid in 87% yield. Though X-ray quality crystals of [**6**][B(C₆F₅)₄] could not be successfully grown, the proposed formulation was unambiguously established through multinuclear 1D and 2D NMR, IR and combustion analysis data. In particular, the ¹H NMR spectrum of **6**⁺ contains a characteristic Me–OAc singlet (δ 3.40 ppm and no signal in the Zn–Me region (Figure 8)). IR data are also in line with the presence of a ZnOAc moiety [ν_{max} (cm⁻¹) = 1616m, 1373w, 1340w]. A Zn(κ²-OAc) coordination is proposed by analogy with neutral Zn–OAc/Zn–O₂CH species.^[26]

For further rationalization, the CO₂ insertion reaction of **5**⁺ (**V**) was DFT computed (BLYP/def2-SVP). As depicted in Figure 9, CO₂ insertion into the Zn–Me bond of **V** is fairly exergonic (ΔΔG = 22.1 kcal/mol) as expected with the formation of two Zn–O bonds in **VI** (Figures S34–S36, Supporting Information). Regarding the reaction profile, an initial interaction of **V** with CO₂ forms **V-CO₂** (ΔG = 6.2 kcal/mol), in which CO₂ is in close vicinity, but not coordinated, to the Zn(II) center (shortest d_{Zn–O} = 3.262 Å). The formation of the CO₂ insertion product **VI** then occurs through a synchronous transition state (**TS2**, Figure S35, Supporting Information) with an overall energy barrier of 24.0 kcal/mol from **V** and free CO₂, in line with a room temperature reaction as observed. **TS2** may be described as a Zn–CO₂ adduct (d_{Zn–O} = 2.177 Å) featuring quite elongated Zn–O=C (d_{C–O} = 1.239 Å) and Zn–Me⁺ (2.184 Å) bonds relative to those in free CO₂ (1.177 Å) and **V** (d_{Zn–Me} = 2.009 Å), respectively. This comes along with a significant bending of the CO₂ moiety (O–C–O = 144.6°). The long Zn–OC/Zn–CH₃ C–C distance in **TS2** (2.136 Å *vs.* 1.513 Å for the C–C bond in **VI**) indicates little C–C bond formation.

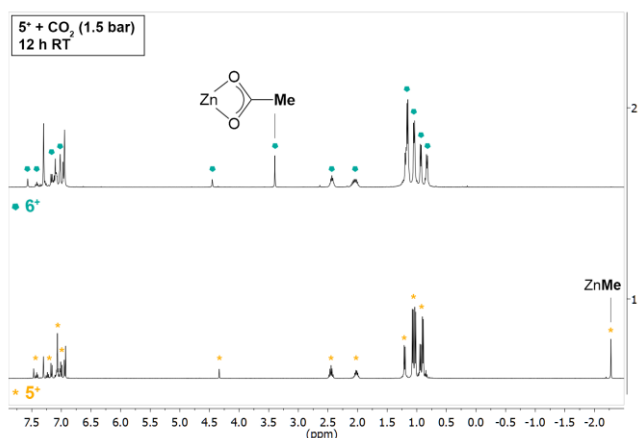
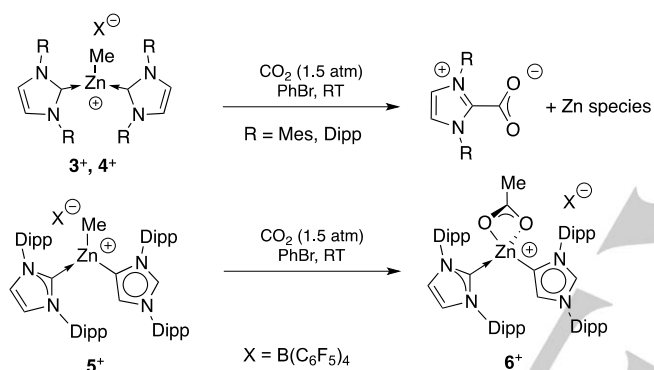


Figure 8. ^1H NMR monitoring of the reaction of 5^+ (bottom) with CO_2 (1.5 bar, $\text{C}_6\text{D}_5\text{Br}$, room temperature) to quantitatively yield Zn-OAc cation 6^+ (top).



Scheme 5. Reactivity of the $(\text{NHC})_2\text{Zn-Me}^+$ cations 3^+ - 5^+ with CO_2 .

The ability of $(\text{NHC})_2\text{ZnMe}^+$ cations to insert CO_2 prompted their use as potential CO_2 hydrosilylation catalysts. Initial studies involved cations $(n\text{NHC})_2\text{ZnMe}^+$ (3^+ - 4^+) which, unsurprisingly, are inactive in CO_2 hydrosilylation catalysis [10 equiv. of $\text{HSi}(\text{OEt})_3$, 1.5 atm. of CO_2 , $\text{C}_6\text{D}_5\text{Br}$, 90 °C, 24 h]. In sharp contrast, cation $(n\text{IDipp})(a\text{IDipp})\text{ZnMe}^+$ (5^+) catalyzes the hydrosilylation of CO_2 (1.5 atm.) in the presence of $\text{HSi}(\text{OEt})_3$ (15 equiv.) to selectively afford the corresponding silylformate product $\text{H-CO}_2\text{-Si}(\text{OEt})_3$ ($\text{C}_6\text{D}_5\text{Br}$, 90 °C, 60h, 90% conversion vs. an internal standard, C_6Me_6), isolated in 76% yield (Scheme 6; Figures S24-S26, Supporting Information).^[34] A NMR-scale control experiment ($\text{C}_6\text{D}_5\text{Br}$, 90 °C, 24h) showed no reaction between an equimolar amount of the Zn-Me cation 5^+ and $\text{HSi}(\text{OEt})_3$, indicating no H/Me exchange reaction of 5^+ prior to CO_2 insertion. Furthermore, isolated Zn-OAc cation 6^+ performed similarly to 5^+ , in line with the former being a catalytic intermediate when starting from 5^+ . Also, no CO_2 hydrosilylation product was observed using IDipp as catalyst ($\text{C}_6\text{D}_5\text{Br}$, 90 °C, 60h), ruling out a NHC-catalyzed process (through dissociation of cation 5^+).^[35] Therefore, under catalytic conditions, cation 5^+ first inserts CO_2 to yield the Zn-OAc cation 6^+ , which then reacts with $\text{HSi}(\text{OEt})_3$

to produce a Zn hydride cation, the presumed catalyst of the CO_2 hydrosilylation reaction.^[12] Such a mechanism has recently been DFT-rationalized in the case of neutral Zn-H catalysts.^[36] Several attempts to generate the putative cation $(n\text{IDipp})(a\text{IDipp})\text{Zn-H}^+$ remained unsuccessful.

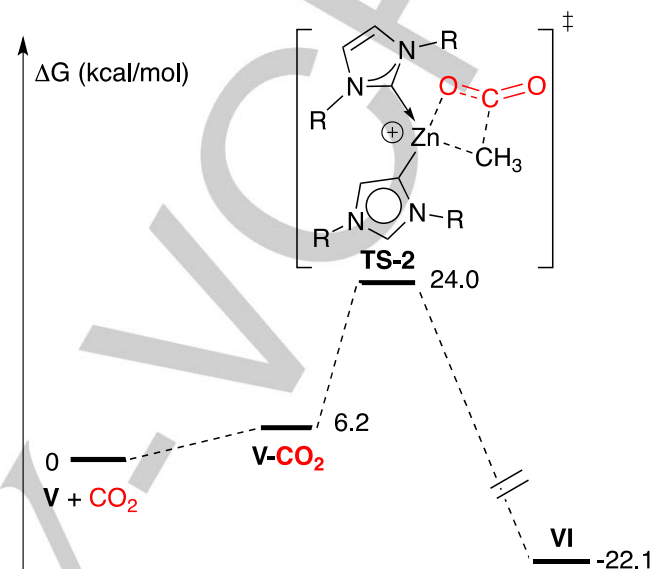
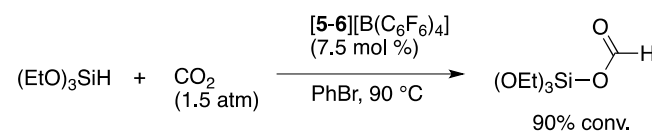


Figure 9. DFT-computed (BLYP/def2-SVP, gas phase) Gibbs free energy (kcal/mol) reaction profile for CO_2 insertion of V .

For comparison, the benchmark Zn-alkyl cation $(\text{Et}_2\text{O})_3\text{Zn-Et}^+$ [as a $\text{B}(\text{C}_6\text{F}_5)_4^-$ salt]^[33] was tested and displayed neither CO_2 insertion reactivity nor catalytic activity ($\text{C}_6\text{D}_5\text{Br}$, room temperature to 100 °C), highlighting the beneficial role of NHC coordination for robust, yet reactive, Zn(II) center. Cation 5^+ is however less active than Zn-H catalysts known thus far,^[12,25d,26] possibly due to greater steric hindrance at Zn(II) in 5^+ .



Scheme 6. Catalytic CO_2 hydrosilylation using cations 5^+ or 6^+ as pre-catalyst.

Summary - Conclusions

Tris-organyl Zn alkyl cations of the type $(\text{NHC})_2\text{ZnMe}^+$ were first accessed and structurally characterized to unveil a coordination chemistry strongly dependent upon sterics, which was favorably exploited for stoichiometric and catalytic CO_2 functionalization through CO_2 insertion chemistry. Thus, while cation $(n\text{IMes})_2\text{ZnMe}^+$ is a stable and robust compound, the severely sterically congested $(n\text{IDipp})_2\text{ZnMe}^+$ undergoes a normal-to-

abnormal NHC isomerization in the presence of THF or free IDipp to afford the most thermodynamically stable isomer $(n\text{IDipp})(a\text{IDipp})\text{ZnMe}^+$, a reaction driven by steric relief despite unfavorable electronics. Combined experimental and DFT data agree with an IDipp-catalyzed isomerization with an initial deprotonation of $(n\text{IDipp})_2\text{ZnMe}^+$.

$n\text{NHC}$ -to- $a\text{NHC}$ isomerization to $(n\text{IDipp})(a\text{IDipp})\text{ZnMe}^+$ was shown to be extremely beneficial for well-behaved reactivity with CO_2 , including the first direct CO_2 insertion into a discrete Zn -alkyl compound. Cation $(n\text{IDipp})(a\text{IDipp})\text{ZnMe}^+$ is a robust tri-organyl Zn -alkyl cation able to act as a CO_2 hydrosilylation pre-catalyst. This shows that Lewis-base-supported cationic Zn -alkyls, a class of readily available electrophilic organometallics *via* well-established synthetic methodologies,^[3] are amenable to CO_2 functionalization catalysis through Zn - R coordination/insertion chemistry. The results detailed herein also further support the use of $a\text{NHC}$ (vs. $n\text{NHC}$) ligation in severely crowded NHC metal complexes for well-behaved reactivity.^[14]

Experimental Section

All experiments were carried out under N_2 using standard Schlenk techniques or in a Mbraun Labmaster I30 glovebox. Toluene, tetrahydrofuran, and pentane were collected after going through drying columns (MB SPS-800), then distilled under N_2 (over Na/benzophenone , or CaH_2), and stored at last for 24 h over molecular sieves (4 Å) in a glovebox prior to use. All deuterated solvents were purchased from Aldrich, excepted for $\text{C}_6\text{D}_5\text{Br}$, purchased from ABCR GmbH & Co. C_6D_6 , CD_2Cl_2 , and d_8 -THF were distilled over CaH_2 , degassed under a N_2 flow, and stored in a glovebox over activated molecular sieves (4 Å) prior to use. Anhydrous $\text{C}_6\text{D}_5\text{Br}$ was stored in a glovebox over activated molecular sieves (4 Å) for 24 h prior to use. ZnMe_2 and $[\text{CPh}_3][\text{B}(\text{C}_6\text{F}_5)_4]$ were purchased from Strem Chemicals Inc. and were used as received. CO_2 was purchased from Linde (HiQ[®] carbon dioxide 4.0 grade 99.99%), and was used after going through drying columns (CoCl_2 and P_2O_5). All other chemicals were purchased from Aldrich and were used as received. The NMR spectra were recorded on Bruker AC 300, 400 or 500 MHz NMR spectrometers in J-Young Teflon valve NMR tube at ambient temperature. Two-dimensional ^1H COSY and ^{13}C - ^1H HSQC correlation experiments were used to assign without ambiguity specific ^1H and ^{13}C NMR resonances of all compounds. IMes ,^[37] IDipp,^[38] IDipp- d_2 ,^[19] $[(\text{IMes})\text{ZnMe}_2]^{[11]}$ and $[(\text{IDipp})\text{ZnMe}_2]^{[11]}$ were prepared according to literature procedures. The salts $[\mathbf{1-2}][\text{B}(\text{C}_6\text{F}_5)_4]$ were generated according to literature.^[11] Crystallographic data were collected using a Bruker KAPPA APEX II DUO diffractometer at the Service de Radiocristallographie of the Institut de Chimie de Strasbourg. Elemental analyses were performed at the Service d'analyses of the Université de Strasbourg. FT-IR spectra were recorded within the region 4000–650 cm^{-1} on a Nicolet 6700 FTIR spectrometer (ATR mode, SMART ORBIT accessory, Ge crystal).

$[(n\text{IMes})_2\text{ZnMe}][\text{B}(\text{C}_6\text{F}_5)_4]$ ($\mathbf{[3]}[\text{B}(\text{C}_6\text{F}_5)_4]$). In a glovebox, a precooled CH_2Cl_2 (5 mL, -40°C) solution of $[\text{CPh}_3][\text{B}(\text{C}_6\text{F}_5)_4]$ (807 mg, 875 μmol) was dropwise added to a CH_2Cl_2 solution of adduct $[(\text{IMes})\text{ZnMe}_2]$ (350 mg, 875 μmol) and 2 equiv. THF (140 μL , 1.75 mmol) and the resulting solution was stirred for 1 h at room temperature. Solid IMes (268 mg, 875 μmol) was then added, and the resulting mixture was allowed to stir, at room temperature, for 30 minutes. Afterward the solution was concentrated to 1/4 of its original volume under reduced pressure. Upon

addition of pentane a white powder formed and was recovered through glass frit filtration. The gathered colorless solid was washed twice with pentane (2 x 10 mL) and dried under *vacuum* (982 mg, 82% yield). Suitable crystals for X-ray diffraction analysis were grown from a saturated toluene solution at -35°C . Elemental analysis for $\text{C}_{67}\text{H}_{51}\text{BF}_{20}\text{N}_4\text{Zn}$ (1368.33): calcd. C 58.81 H 3.76 N 4.09; found C 58.85 H 3.92 N 4.03. ^1H NMR (CD_2Cl_2 , 500 MHz): δ -1.35 (s, 3H, Zn-CH_3), 1.71 (s, 24H, Mes-CH_3), 2.42 (s, 12H, Mes-CH_3), 6.92 (s, 8H, CH-Ar), 7.02 (s, 4H, NCHCHN) ppm. $^{13}\text{C}\{^1\text{H}\}$ NMR (CD_2Cl_2 , 125 MHz): δ -7.4 (Zn-CH_3), 17.5 ($o\text{-CH}_3$), 21.3 ($p\text{-CH}_3$), 124.6 (NCHCHN), 130.0 (Ar), 130.1 ($\text{C}_{ipso}\text{-B}(\text{C}_6\text{F}_5)_4$), 134.2 (Ar), 135.1 (Ar), 136.7 (d, $^1J_{\text{C,F}} = 241$ Hz, $\text{B}(\text{C}_6\text{F}_5)_4$), 138.6 (d, $^1J_{\text{C,F}} = 246$ Hz, $\text{B}(\text{C}_6\text{F}_5)_4$), 140.5 (Ar), 148.5 (d, $^1J_{\text{C,F}} = 241$ Hz, $\text{B}(\text{C}_6\text{F}_5)_4$), 177.0 (Zn-C_{NHC}) ppm. ^{19}F NMR (292 MHz, $\text{C}_6\text{D}_5\text{Br}$): δ -167.1 (dd, 8F, $^3J_{\text{F,F}} = 21.0$ Hz, $^3J_{\text{F,F}} = 16.0$ Hz, $o\text{-C}_6\text{F}_5$), -163.3 (t, 4F, $^3J_{\text{F,F}} = 21.0$ Hz, $p\text{-C}_6\text{F}_5$), -132.7 (d, 8F, $^3J_{\text{F,F}} = 16.0$ Hz, $m\text{-C}_6\text{F}_5$) ppm; ^{11}B NMR (128 MHz, $\text{C}_6\text{D}_5\text{Br}$): δ -15.9 (s, 1B, $\text{B}(\text{C}_6\text{F}_5)_4$) ppm.

$[(n\text{IDipp})_2\text{ZnMe}][\text{B}(\text{C}_6\text{F}_5)_4]$ ($\mathbf{[4]}[\text{B}(\text{C}_6\text{F}_5)_4]$). In a glovebox, a precooled toluene (15 mL, -35°C) solution of $[\text{CPh}_3][\text{B}(\text{C}_6\text{F}_5)_4]$ (572 mg, 620 μmol) was dropwise added to a mixture of adduct $[(\text{IDipp})\text{ZnMe}_2]$ (300 mg, 620 μmol) and 2 equiv. THF (100 μL , 1.25 mmol) in toluene (15 mL, -35°C). Carbene IDipp (242 mg, 620 μmol) was then added all at once as a solid. The resulting mixture immediately became a pale yellow solution and was allowed to stir at room temperature for 10 min. Afterward, the volatiles were removed under reduced pressure and the crude solid washed with pentane (4 x 10 mL) to yield, according to ^1H and ^{13}C NMR data, pure salt $[\mathbf{4}][\text{B}(\text{C}_6\text{F}_5)_4]$ as a beige solid (78% yield). Suitable crystals for X-ray diffraction analysis and elemental analysis were grown from a toluene solution layered with pentane at -35°C . Elemental analysis for $\text{C}_{79}\text{H}_{75}\text{BF}_{20}\text{N}_4\text{Zn}$ (1536.65): calcd. C 61.75 H 4.92 N 3.65; found C 61.29 H 5.12 N 3.24. ^1H NMR ($\text{C}_6\text{D}_5\text{Br}$, 500 MHz): δ -0.91 (s, 3H, Zn-CH_3), 0.82 (d, $^3J = 6.9$ Hz, 24H, $\text{CH}_3\text{-}i\text{Pr}$), 0.85 (d, $^3J = 6.9$ Hz, 24H, $\text{CH}_3\text{-}i\text{Pr}$), 2.32 (hept, $^3J = 6.9$ Hz, 8H, $\text{CH-}i\text{Pr}$), 6.75 (s, 4H, -CH=CH-), 6.97 (d, $^3J = 7.9$ Hz, 8H, CH-Ar), 7.30 (t, $^3J = 7.9$ Hz, 4H, CH-Ar) ppm. ^{13}C NMR ($\text{C}_6\text{D}_5\text{Br}$, 125 MHz): δ -2.6 (Zn-CH_3), 22.0 ($i\text{Pr}$), 25.0 ($i\text{Pr}$), 28.4 ($i\text{Pr}$), 124.7 (NCHCHN), 125.6 (Ar), 131.0 (Ar), 133.7 (Ar), 136.4 (d, $^1J_{\text{C,F}} = 241$ Hz, $\text{B}(\text{C}_6\text{F}_5)_4$), 138.3 (d, $^1J_{\text{C,F}} = 238$ Hz, $\text{B}(\text{C}_6\text{F}_5)_4$), 144.8 (Ar), 148.5 (d, $^1J_{\text{C,F}} = 243$ Hz, $\text{B}(\text{C}_6\text{F}_5)_4$), 178.9 (Zn-C_{NHC}) ppm. ^{19}F NMR ($\text{C}_6\text{D}_5\text{Br}$, 292 MHz): δ -132.4 (d, $^3J_{\text{F,F}} = 11$ Hz, 8F, $o\text{-C}_6\text{F}_5$), -163.0 (t, $^3J_{\text{F,F}} = 21$ Hz, 4F, $p\text{-C}_6\text{F}_5$), -166.8 (dd, $^3J_{\text{F,F}} = 21$ Hz, $^3J_{\text{F,F}} = 11$ Hz, 8F, $m\text{-C}_6\text{F}_5$) ppm. ^{11}B NMR ($\text{C}_6\text{D}_5\text{Br}$, 128 MHz): δ -16.2 (s, 1B, $\text{B}(\text{C}_6\text{F}_5)_4$) ppm.

$[(\text{IDipp-}d_2)_2\text{ZnMe}][\text{B}(\text{C}_6\text{F}_5)_4]$ ($\mathbf{[4-d]}[\text{B}(\text{C}_6\text{F}_5)_4]$). This salt was prepared following the same procedure than that for $[\mathbf{4}][\text{B}(\text{C}_6\text{F}_5)_4]$ but using IDipp- d_2 as a carbene source. ^2H NMR ($\text{C}_6\text{H}_5\text{Br}$, 500 MHz): δ 6.77 (s, 4H, NCDCDN) ppm.

$[(a\text{IDipp})(n\text{IDipp})\text{ZnMe}][\text{B}(\text{C}_6\text{F}_5)_4]$ ($\mathbf{[5]}[\text{B}(\text{C}_6\text{F}_5)_4]$). Salt $[\mathbf{4}][\text{B}(\text{C}_6\text{F}_5)_4]$ (762 mg, 0.496 mmol) was dissolved in THF (10 mL) and the resulting off-white solution was stirred at room temperature for 48 h. The reaction was monitored by ^1H NMR spectroscopy (through NMR analysis of aliquots) showing the complete conversion of $[\mathbf{4}][\text{B}(\text{C}_6\text{F}_5)_4]$ to $[\mathbf{5}][\text{B}(\text{C}_6\text{F}_5)_4]$ after 48h. After this time the solution was concentrated under reduced pressure to 1/4 of its original volume. Upon addition of pentane a light brown powder formed. Trituration with a toluene/pentane (1:10) mixture allowed, after drying under vacuum, the isolation of salt $[\mathbf{5}][\text{B}(\text{C}_6\text{F}_5)_4]$ as a beige powder in a pure form (587 mg, 77% yield). Suitable crystals for X-ray diffraction analysis were grown from a saturated toluene solution at -35°C . Elemental analysis for $\text{C}_{79}\text{H}_{75}\text{BF}_{20}\text{N}_4\text{Zn}$ (1536.65): calcd. C 61.75 H 4.92 N 3.65; found C 61.41 H 5.00 N 3.29. ^1H NMR ($\text{C}_6\text{D}_5\text{Br}$, 300 MHz): δ -2.28 (s, 3H, Zn-CH_3), 0.90 (d, $^3J = 6.9$ Hz, 12H, $\text{CH}_3\text{-}i\text{Pr}$), 0.94 (d, $^3J = 6.8$ Hz, 6H, $\text{CH}_3\text{-}i\text{Pr}$), 1.02 (d, $^3J = 6.9$ Hz, 12H, $\text{CH}_3\text{-}i\text{Pr}$), 1.07 (d, $^3J = 6.9$ Hz, 12H, $\text{CH}_3\text{-}i\text{Pr}$), 1.20 (d, $^3J = 6.8$ Hz, 6H, $\text{CH}_3\text{-}i\text{Pr}$), 1.95-2.08 (m, 4H, $\text{CH-}i\text{Pr}$), 2.45 (sept, $^3J = 6.8$ Hz, 4H, $\text{CH-}i\text{Pr}$), 4.33 (s, 1H, NCCHN),

6.93 (s, 2H, NCHCHN), 7.00 (d, $^3J = 7.9$ Hz, 2H, CH-Ar), 7.05-7.09 (m, 6H, CH-Ar), 7.17 (d, $^3J = 7.9$ Hz, 2H, CH-Ar), 7.24 (t, $^3J = 7.9$ Hz, 1H, CH-Ar), 7.42 (t, $^3J = 7.9$ Hz, 1H, CH-Ar), 7.46 (br s, 1H, NCHN) ppm. $^{13}\text{C}\{^1\text{H}\}$ NMR ($\text{C}_6\text{D}_5\text{Br}$, 75 MHz): δ -9.9 (Zn-CH₃), 22.9 (iPr), 23.0 (iPr), 23.5 (iPr), 23.7 (iPr), 24.5 (iPr), 24.9 (iPr), 28.2 (iPr), 28.3 (iPr), 28.6 (iPr), 123.9 (Ar), 124.1 (Ar), 124.4 (Ar), 124.6 (NCHCHN), 129.7 (Ar), 130.5 (NCCHN), 130.6 (Ar), 131.2 (Ar), 132.8 (Ar), 134.7 (Ar), 136.4 (d, $^1J_{\text{C,F}} = 241$ Hz, B(C₆F₅)₄), 136.4 (NCHN), 138.1 (d, $^1J_{\text{C,F}} = 238$ Hz, B(C₆F₅)₄), 144.2 (Ar), 144.3 (Ar), 145.1 (Ar), 148.5 (d, $^1J_{\text{C,F}} = 242$ Hz, B(C₆F₅)₄), 154.7 (Zn-C_{ANHC}), 178.7 (Zn-C_{7NHC}) ppm. ^{19}F NMR ($\text{C}_6\text{D}_5\text{Br}$, 292 MHz): δ -132.7 (d, $^3J_{\text{F,F}} = 11$ Hz, 8F, o-C₆F₅), -163.3 (t, $^3J_{\text{F,F}} = 21$ Hz, 4F, p-C₆F₅), -167.1 (dd, $^3J_{\text{F,F}} = 21$ Hz, $^3J_{\text{F,F}} = 11$ Hz, 8F, m-C₆F₅) ppm. ^{11}B NMR (128 MHz, $\text{C}_6\text{D}_5\text{Br}$): δ -15.9 (s, 1B, B(C₆F₅)₄) ppm. FT-IR ν_{max} (solid)/cm⁻¹: 1642w, 1546w, 1513m, 1463s, 1367vw, 1330w, 1275w, 1085m, 980s, 803w, 756m, 683w, 661w.

[(alDipp-d₂)(nlDipp-d₂)ZnMe][B(C₆F₅)₄] ([5-d₄][B(C₆F₅)₄]). This salt was generated on a NMR-scale through the IDipp-mediated isomerization of cation **4-d₄⁺**. A ^2H NMR analysis showed the complete conversion to **5-d₄⁺**. ^2H NMR ($\text{C}_6\text{H}_5\text{Br}$, 500 MHz): δ 4.33 (br s, 1D, -CD-CZn-), 6.94 (s, 2D, -CD=CD-), 7.46 (br s, 1H, -N-CD-N-) ppm.

[(alDipp)(IDipp)Zn(OAc)][B(C₆F₅)₄] ([6][B(C₆F₅)₄]). Complex **[5][B(C₆F₅)₄]** (40 mg, 26 μmol) was dissolved in 0.6 mL *d*₅-bromobenzene and placed in a J-Young Teflon valve NMR tube. The latter was charged with carbon dioxide (1.5 atm) and the CO₂ insertion reaction was monitored by ^1H NMR with a complete conversion to **[6][B(C₆F₅)₄]** after 12 h. Complex **[6][B(C₆F₅)₄]** was isolated as a light brown powder after precipitation in cold pentane (20 mL), removal of the solvents after decantation and drying under vacuum (36 mg, 87% yield). Elemental analysis for C₈₀H₇₅BF₂₀N₄O₂Zn·2(C₆D₅Br) (1894.68): calcd. C 58.31 H 4.54 N 2.96; found C 58.35 H 4.63 N 3.21. ^1H NMR ($\text{C}_6\text{D}_5\text{Br}$, 500 MHz): δ 0.83 (d, $^3J = 6.7$ Hz, 6H, CH₃-iPr), 0.93 (d, $^3J = 6.8$ Hz, 6H, CH₃-iPr), 1.05 (d, $^3J = 6.9$ Hz, 12H, CH₂-iPr), 1.16 (m, 24H, CH₂-iPr), 1.93-2.15 (m, 4H, CH-iPr), 2.43 (sept, $^3J = 6.9$ Hz, 4H, CH-iPr), 3.40 (s, OAc), 4.45 (s, 1H, NCHCHN), 6.97 (s, 2H, NCHCHN), 7.02-7.14 (m, 8H, CH-Ar), 7.17 (d, $^3J = 7.7$ Hz, 2H, CH-Ar), 7.28 (t, $^3J = 7.9$ Hz, 1H, CH-Ar), 7.42 (t, $^3J = 7.8$ Hz, 1H, CH-Ar), 7.57 (br s, 1H, NCHN) ppm (s, 2H, CH-Ar). $^{13}\text{C}\{^1\text{H}\}$ NMR ($\text{C}_6\text{D}_5\text{Br}$, 75 MHz): δ 21.4 (iPr), 21.6 (iPr), 22.9 (iPr), 23.0 (iPr), 23.2 (iPr), 23.5 (CH₃-OAc), 23.9 (iPr), 24.0 (iPr), 24.4 (iPr), 25.6 (iPr), 28.2 (iPr), 28.4 (iPr), 28.5 (iPr), 28.7 (iPr), 28.8 (iPr), 28.9 (iPr), 123.7 (Ar), 123.9 (Ar), 124.3 (Ar), 124.4 (Ar), 124.7 (NCHCHN), 124.9 (Ar), 125.2 (Ar), 128.1 (Ar), 128.9 (Ar), 130.4 (NCCHN), 130.5 (Ar), 131.3 (Ar), 131.9 (Ar), 132.5 (Ar), 133.3 (Ar), 133.5 (Ar), 136.4 (d, $^1J_{\text{C,F}} = 235.1$ Hz, B(C₆F₅)₄), 137.4 (NCHN), 138.3 (d, $^1J_{\text{C,F}} = 240.0$ Hz, B(C₆F₅)₄), 144.3 (Ar), 144.4 (Ar), 144.5 (Ar), 144.5 (Ar), 144.8 (Ar), 145.5 (Ar), 145.6 (Ar), 145.7 (Ar), 148.0 (Ar), 148.5 (d, $^1J_{\text{C,F}} = 243$ Hz, B(C₆F₅)₄), 162.8 (Zn-C_{ANHC}), 171.5 (C=O), 172.6 (Zn-C_{7NHC}) ppm. FT-IR ν_{max} (solid)/cm⁻¹: 1648m, 1616m (OAc), 1540w, 1512m, 1463s, 1373w (OAc), 1340w (OAc), 1330sh, 1275w, 1085m, 1061w, 1014w, 979s, 804w, 774w, 756m, 683w, 661w.

Kinetic studies of the conversion of 4⁺ to 5⁺. All kinetic runs were performed on the NMR scale allowing a direct monitoring of the rearrangement reaction by ^1H NMR. Each was prepared in a glove box as follows: a 0.06M solution of cation **4⁺** in $\text{C}_6\text{D}_5\text{Br}$ (0.5 mL) was charged in a J-Young Teflon valve NMR tube with the desired amount of IDipp (0.2 equiv. vs. **4⁺**). Setup analysis (for kinetic studies) of the NMR spectrometer allowed the first ^1H NMR spectrum to be recorded approximately 15 min after sample preparation. Subsequent ^1H NMR spectra were recorded every 90s for several hours. The conversion of **4⁺** to **5⁺** was estimated via integration of the ^1H signals of the Zn-Me moiety and the appearance of the CHCZn upfield signal (δ 4.33 ppm, s, 1H) for cation **5⁺**. The dependence of the reaction rate on [IDipp] and **4⁺** was determined through the initial rates method. Rate dependence on IDipp:

for a given **4⁺**, the kinetic study was done with four different concentrations of free IDipp (**4⁺**]₀ = 1.74×10⁻² M; [IDipp]₀ = 0.43×10⁻², 0.87×10⁻², 1.31×10⁻² and 1.74×10⁻² M). Rate dependence on cation **4⁺**: for a given [IDipp]₀, the kinetic study was done with four different concentrations of **4⁺** ([IDipp]₀ = 1.74×10⁻² M; **4⁺**]₀ = 1.05×10⁻², 1.74×10⁻², 2.40×10⁻² and 3.14×10⁻² M). Initial reaction rates were approximated from a 3% conversion to **5⁺**.

Typical procedure for the hydrosilylation of CO₂ with HSi(OEt)₃ catalyzed by [5][B(C₆F₅)₄] and [6][B(C₆F₅)₄]. Complex **[5][B(C₆F₅)₄]** (1 equiv.), HSi(OEt)₃ (10 to 20 equiv.), and hexamethylbenzene (1-13 equiv., used as an internal standard), were dissolved in 0.6 mL of *d*₅-bromobenzene and placed in a J-Young Teflon valve NMR tube. The NMR tube was charged with CO₂ (1.5 atm) and placed in an oil bath preheated at 90 °C. The conversion of the silane [(EtO)₃Si-H: δ 4.45 ppm in $\text{C}_6\text{D}_5\text{Br}$] to silyl formate [(EtO)₃Si-OC(O)-H: δ 7.98 ppm in $\text{C}_6\text{D}_5\text{Br}$] was monitored by ^1H NMR. Complex **[5][B(C₆F₅)₄]** (10.5 mg, 6.83 μmol , 1 equiv.; internal standard: C₆Me₆, 11 mg, 68.3 μmol , 10 equiv.) hydrosilylated CO₂ with 90% conv. of (EtO)₃SiH (19 μL , 103 μmol , 15 equiv.) to triethoxysilyl formate H-CO₂-Si(OEt)₃ within 60 h at 90 °C. H-CO₂-Si(OEt)₃ was isolated in a pure form (as checked by ^1H NMR) in 76% yield by distillation under reduced pressure.^[26] Increasing the catalyst loading [10% mol. vs. (EtO)₃SiH] led to the quantitative formation of H-CO₂-Si(OEt)₃ after 48 h (90 °C, $\text{C}_6\text{D}_5\text{Br}$). When starting from the Zn-OAc⁺ cation **6⁺**, i.e. salt **[6][B(C₆F₅)₄]**, a nearly identical catalytic activity was observed. No catalytic activity was observed upon using HSiEt₃ (10 equiv.) as a silane source (90 °C, $\text{C}_6\text{D}_5\text{Br}$, 48 h).

Supporting Information

NMR data for all prepared species, crystal data and refinement for compounds **[3-6][B(C₆F₅)₄]** (CCDC numbers 1416946-48, respectively), detailed NBO analysis for cations **3⁺**, **4⁺** and **5⁺**, kinetic data and associated plots and NMR data for the conversion of **4⁺** to **5⁺**, molecular structures of all compounds/intermediates modeled through DFT studies. The Cartesian coordinates of all computed molecules.

Acknowledgements

The authors thank the CNRS and the University of Strasbourg for financial support. C.F. thanks the *Fundação para a Ciência e Tecnologia* (FCT), Portugal, for a post-doc fellowship (SFRH/BPD/73253/2010). J.C.B. is grateful to the French ministry of research for a Ph.D fellowship.

Keywords: N-heterocyclic carbene • zinc • cation • CO₂ insertion • hydrosilylation ,

- [1] T. Hirose, K. Kodama, in *Comprehensive Organic Synthesis*, eds. P. Knochel, G. A. Molander, Elsevier B. V., Amsterdam, 2nd edition, 2014, Vol. 1, pp 204-266.
- [2] For early reports on Zn(II) alkyl cations, see: a) R. M. Fabicon, A. D. Pajerski, H. G. Richey, *J. Am. Chem. Soc.* 1991, 113, 6680; b) H. Tang, H. G. Richey, *Organometallics* 1996, 15, 4891.
- [3] For representative examples, see: a) M. Haufe, R. D. Köhn, R. Weimann, G. Seifert, D. Zeigan, *J. Organomet. Chem.* 1996, 520, 121; b) H. Tang, M. Parvez, H. G. Richey, *Organometallics* 2000, 19, 4810; c) D. A. Walker, T. J. Woodman, D. L. Hughes, M. Bochmann, *Organometallics* 2001, 20, 3772; d) M. D. Hannant, M. Schormann, M.

- Bochmann, *J. Chem. Soc., Dalton Trans.* **2002**, 4071; e) D. A. Walker, T. J. Woodman, M. Schormann, D. L. Hughes, M. Bochmann, *Organometallics* **2003**, *22*, 797; f) M. Bochmann, *Coord. Chem. Rev.* **2009**, *253*, 2000; g) C. A. Wheaton, B. J. Ireland, P. G. Hayes, *Organometallics* **2009**, *28*, 1282; h) C. A. Wheaton, P. G. Hayes, *Chem. Commun.* **2010**, *46*, 8404; i) M. A. Chilleck, T. Braun, B. Braun, S. Mebs, *Organometallics* **2014**, *33*, 551.
- [4] a) R. J. Wehmschulte, L. Wojtas, *Inorg. Chem.* **2011**, *50*, 11300; b) T. O. Petersen, E. Tausch, J. Schaefer, H. Scherer, P. W. Roesky, I. Krossing, *Chem. Eur. J.* **2015**, *21*, 13696; c) T. A. Engesser, C. Friedmann, A. Martens, D. Kratzert, P. J. Malinowski, I. Krossing, *Chem. Eur. J.* **2016**, *22*, 15085.
- [5] a) M. A. Chilleck, L. Hartenstein, T. Braun, P. W. Roesky, B. Braun, *Chem. Eur. J.* **2015**, *21*, 2594; b) K. Freitag, H. Banh, C. Ganesamoorthy, C. Gemel, R. W. Seidel, R. A. Fischer, *Dalton Trans.* **2013**, *42*, 10540; c) M. A. Chilleck, T. Braun, B. Braun, *Chem. Eur. J.* **2011**, *17*, 12902.
- [6] a) A. Lühl, H. P. Nayek, S. Blechert, P. W. Roesky, *Chem. Commun.* **2011**, *47*, 8280; b) C. Romain, V. Rosa, C. Fliedel, F. Bier, F. Hild, R. Welter, S. Dagorne, T. Avilés, *Dalton Trans.* **2012**, *41*, 3377; c) Y. Sarazin, J.-F. Carpentier, *Chem. Rev.* **2015**, *115*, 3564.
- [7] M. Khandelwal, R. J. Wehmschulte, *Angew. Chem. Int. Ed.* **2012**, *51*, 7323; *Angew. Chem.* **2012**, *29*, 7435.
- [8] Selected reviews/books: a) N-Heterocyclic Carbenes: Effective Tools in Organometallic Synthesis (Ed.: S. P. Nolan), Wiley-VCH, Weinheim, **2014**; b) D. Bourissou, O. Guerret, F. Gabbai, G. Bertrand, *Chem. Rev.* **2000**, *100*, 39; c) W. A. Herrmann, *Angew. Chem. Int. Ed.* **2002**, *41*, 1290; *Angew. Chem.* **2002**, *114*, 1342; d) V. César, S. Bellemin-Lapponnaz, L. H. Gade, *Chem. Soc. Rev.* **2004**, *33*, 619; e) P. de Frémont, N. Marion, S. P. Nolan, *Coord. Chem. Rev.* **2009**, *253*, 862; f) C. Fliedel, G. Schnee, T. Avilés, S. Dagorne, *Coord. Chem. Rev.* **2014**, *275*, 63; g) S. Bellemin-Lapponnaz, S. Dagorne, *Chem. Rev.* **2014**, *114*, 8747.
- [9] For a review on NHC-supported group 12 metals, see: S. Budagumpi, S. Endud, *Organometallics* **2013**, *32*, 1537.
- [10] a) P. Jochmann, D. W. Stephan, *Chem. Eur. J.* **2014**, *20*, 8370; b) O. Jacquet, X. Frogneux, C. Das Neves Gomes, T. Cantat, *Chem. Sci.* **2013**, *4*, 2127; c) C. Fliedel, D. Vila-Viçosa, M. J. Calhorda, S. Dagorne, T. Avilés, *ChemCatChem.* **2014**, *6*, 1357; d) Y. Lee, B. Li, A. H. Hoveyda, *J. Am. Chem. Soc.* **2009**, *131*, 11625; e) T. R. Jensen, L. E. Breyfogle, M. A. Hillmyer, W. B. Tolman, *Chem. Commun.* **2004**, 2504.
- [11] G. Schnee, C. Fliedel, T. Avilés and S. Dagorne, *Eur. J. Inorg. Chem.*, **2013**, 3699.
- [12] a) A. Rit, A. Zanardi, T. P. Spaniol, L. Maron, J. Okuda, *Angew. Chem. Int. Ed.* **2014**, *53*, 13273; *Angew. Chem.* **2014**, *126*, 13489; b) P. A. Lummis, M. R. Momeni, M. W. Lui, R. McDonald, M. J. Ferguson, M. Miskolzie, A. Brown, E. Rivard, *Angew. Chem. Int. Ed.* **2014**, *53*, 9347; *Angew. Chem.* **2014**, *126*, 9501.
- [13] For other purely organometallic Zn cations combining σ - and π -donor ligands, see refs. 4 and 5.
- [14] For reviews on σ -NHC metal complexes, see: a) R. H. Crabtree, *Coord. Chem. Rev.* **2013**, *257*, 755; b) K. F. Donnelly, A. Petronilho, M. Albrecht, *Chem. Commun.* **2013**, *49*, 1145; c) O. Schuster, L. Yang, H. G. Raubenheimer, M. Albrecht, *Chem. Rev.* **2009**, *109*, 3445.
- [15] D. Tapu, D. A. Dixon, C. Roe, *Chem. Rev.* **2009**, *109*, 3385.
- [16] For well-identified σ -NHC-to- π -NHC isomerization in metal complexes and associated reactivity studies, see: a) P. L. Arnold, S. T. Liddle, *Organometallics* **2006**, *25*, 1485; b) C. E. Cooke, M. C. Jennings, R. K. Pomeroy, J. A. C. Clyburne, *Organometallics* **2007**, *26*, 6059; c) A.-L. Schmitt, G. Schnee, R. Welter, S. Dagorne, *Chem. Commun.* **2010**, *46*, 2480; d) D. Holschumacher, T. Bannenberg, C. G. Hrib, P. G. Jones, M. Tamm, *Angew. Chem. Int. Ed.* **2008**, *47*, 7428; *Angew. Chem.* **2008**, *120*, 7538; e) R. A. Musgrave, R. S. P. Tuberville, M. Irwin, J. M. Goicoechea, *Angew. Chem. Int. Ed.* **2012**, *51*, 10832; *Angew. Chem.* **2012**, *124*, 10990; f) B. M. Day, T. Pugh, D. Hendriks, C. Fonseca Guerra, D. J. Evans, F. M. Bickelhaupt, R. A. Layfield, *J. Am. Chem. Soc.* **2013**, *135*, 13338; g) M. Uzelac, A. Hernán-Gómez, D. R. Armstrong, A. R. Kennedy, E. Hevia, *Chem. Sci.* **2015**, *6*, 5719; h) G. Schnee, O. N. Faza, D. Specklin, B. Jacques, L. Karmazin, R. Welter, C. S. López, S. Dagorne, *Chem. Eur. J.* **2015**, *21*, 17959; i) M. Uzelac, D. R. Armstrong, A. R. Kennedy, E. Hevia, *Chem. Eur. J.* **2016**, *22*, 15826.
- [17] For known σ -NHC-Zn species, see ref. 10a and: a) Y. Wang, Y. Xie, M. Y. Abraham, R. J. Gilliard Jr., P. Wei, C. F. Campana, H. F. Schaefer III, P. v. R. Schleyer, G. H. Robinson, *Angew. Chem. Int. Ed.* **2012**, *51*, 10173; *Angew. Chem.* **2012**, *124*, 10320; b) T. K. Sen, S. C. Sau, A. Mukherjee, P. K. Hota, S. K. Mandal, B. Maity, D. Koley, *Dalton Trans.* **2013**, *42*, 14253; c) J. B. Waters, R. S. P. Tuberville, J. M. Goicoechea, *Organometallics* **2013**, *32*, 5190.
- [18] For related and thorough studies on the influence of steric strain on thermodynamic, see refs. 15f, 15g and: a) N. Burford, J. A. C. Clyburne, M. S. W. Chan, *Inorg. Chem.* **1997**, *36*, 3204; b) N. Burford, C. L. B. Macdonald, K. N. Robertson, T. S. Cameron, *Inorg. Chem.* **1996**, *35*, 4013; c) N. Burford, J. A. C. Clyburne, S. Mason, *Inorg. Chem.* **1993**, *32*, 4988.
- [19] For the synthesis of carbene IDipp- d_2 , see: R. M. Stolley, H. A. Duong, J. Louie, *Organometallics* **2013**, *32*, 4952.
- [20] For representative examples of NHCs as strong H-bond acceptors, see: a) S. D. Sarkar, S. Grimme, A. Studer, *J. Am. Chem. Soc.* **2010**, *132*, 1190; b) J. A. Cowan, J. A. C. Clyburne, M. G. Davidson, R. L. W. Harris, J. A. K. Howard, P. Küpper, M. A. Leech, S. P. Richards, *Angew. Chem. Int. Ed.* **2002**, *41*, 1432; *Angew. Chem.* **2002**, *114*, 1490.
- [21] For C-H...C hydrogen bonds with a NHC acting as a H-bond acceptor see: a) A. J. Arduengo III, S. F. Gamper, M. Tamm, J. C. Calabrese, F. Davidson, H. A. Craig, *J. Am. Chem. Soc.* **1995**, *117*, 572; b) L. A. Leites, G. I. Magdanurov, S. S. Bukalov, R. West, *Mendeleev Commun.* **2008**, *18*, 14.
- [22] a) O. Back, M. A. Celik, G. Frenking, M. Melaimi, B. Donnadieu, G. Bertrand, *J. Am. Chem. Soc.* **2010**, *132*, 10262; b) Y. Wang, Y. Xie, M. Y. Abraham, P. Wei, H. F. Schaefer III, P. v. R. Schleyer, G. H. Robinson, *J. Am. Chem. Soc.* **2010**, *132*, 14370.
- [23] D. R. Armstrong, S. E. Baillie, V. L. Blair, N. G. Chabloy, J. Diez, J. Garcia-Alvarez, A. R. Kennedy, S. D. Robertson, E. Hevia, *Chem. Sci.* **2013**, *4*, 4259.
- [24] Recent reviews on metal-catalyzed CO₂ hydrosilylation and hydroboration: a) S. Bontemps, *Coord. Chem. Rev.* **2016**, *308*, 117; b) S. Chakraborty, P. Bhattacharya, H. Dai, H. Guan, *Acc. Chem. Res.* **2015**, *48*, 1995; c) C. C. Chong, R. Kinjo, *ACS Catalysis* **2015**, *5*, 3238; d) A. Tlili, E. Blondiaux, X. Frogneux, T. Cantat, *Green Chem.* **2015**, *17*, 157; e) F. J. Fernández-Alvarez, A. M. Aitani, L. A. Oro, *Catal. Sci. Technol.* **2014**, *4*, 611; f) L. Zhang, Z. Hou, *Chem. Sci.* **2013**, *4*, 3395.
- [25] Recent representative examples of metal-based CO₂ hydro-silylation/hydroboration catalysis: a) S. Chakraborty, J. Zhang, J. A. Krause, H. Guan, *J. Am. Chem. Soc.* **2010**, *132*, 8872; b) S. Park, D. Bézier, M. Brookhart, *J. Am. Chem. Soc.* **2012**, *134*, 11404; c) R. Lalrempuia, M. Iglesias, V. Polo, P. J. Sanz Miguel, F. J. Fernández-Alvarez, J. J. Pérez-Torrente, L. A. Oro, *Angew. Chem. Int. Ed.* **2012**, *51*, 12824; *Angew. Chem.* **2012**, *124*, 12996; d) W. Sattler, G. Parkin, *J. Am. Chem. Soc.* **2012**, *134*, 17462; e) S. J. Mitton, L. Turculet, *Chem. Eur. J.* **2012**, *18*, 15258; f) L. Zhang, J. Cheng, Z. Hou, *Chem. Commun.* **2013**, *49*, 4782; g) R. Shintani, K. Nozaki, *Organometallics* **2013**, *32*, 2459; h) F. A. LeBlanc, W. E. Piers, M. Parvez, *Angew. Chem. Int. Ed.* **2014**, *53*, 789; *Angew. Chem.* **2014**, *126*, 808; i) M. D. Anker, M. Arrowsmith, P. Bellham, M. S. Hill, G. Kociok-Köhn, D. J. Liptrot, M. F. Mahon, C. Weetman, *Chem. Sci.* **2014**, *5*, 2826; j) M. L. Scheuermann, S. P. Semproni, I. Pappas, P. J. Chirik, *Inorg. Chem.* **2014**, *53*, 9463; k) E. Feghali, O. Jacquet, P. Thuéry, T. Cantat, *Catal. Sci. Technol.* **2014**, *4*, 2230; l) G. Jin, C. G. Werncke, Y. Escudí, S. Sabo-Etienne, S. Bontemps, *J. Am. Chem. Soc.* **2015**, *137*, 9563; m) S. Bagherzadeh, N. P. Mankad, *J. Am. Chem. Soc.* **2015**, *137*, 10898; n) D. Mukherjee, S. Shirase, T. P. Spaniol, K. Mashima, J. Okuda, *Chem. Commun.* **2016**,

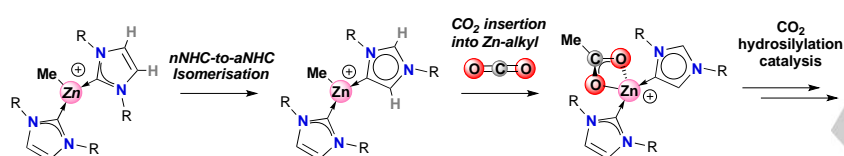
- 52, 13155; o) D. Mukherjee, H. Osseili, T. P. Spaniol, J. Okuda, *J. Am. Chem. Soc.* **2016**, *138*, 10790; p) P. Ríos, J. Diez, J. López-Serrano, A. Rodríguez, S. Conejero, *Chem. Eur. J.* **2016**, *22*, 16791; q) J. Chen, L. Falivene, L. Caporaso, L. Cavallo, E. Y.-X. Chen, *J. Am. Chem. Soc.* **2016**, *138*, 5321; r) A. Julián, E. A. Jaseer, K. Garcés, F. J. Fernández-Alvarez, P. García-Orduña, F. J. Lahoz, L. A. Oro, *Catal. Sci. Technol.* **2016**, *6*, 4410; s) A. Aloisi, J.-C. Berthet, C. Genre, P. Thuéry, T. Cantat, *Dalton Trans.* **2016**, *45*, 14774.
- [26] W. Sattler, G. Parkin, *J. Am. Chem. Soc.* **2011**, *133*, 9708.
- [27] For well-identified CO₂ insertion into a Zn–H bond, see also: a) S. Schulz, T. Eisenmann, S. Schmidt, D. Bläser, U. Westphal, R. Boese, *Chem. Commun.* **2010**, *46*, 7226; b) D. Mukherjee, N. L. Lampland, K. Yan, J. F. Dunne, A. Ellern, A. D. Sadow, *Chem. Commun.* **2013**, *49*, 4334; c) A. Rit, T. P. Spaniol, L. Maron, J. Okuda, *Angew. Chem. Int. Ed.* **2013**, *52*, 4664; *Angew. Chem.* **2013**, *125*, 4762; d) N. J. Brown, J. E. Harris, X. Yin, I. Silverwood, A. J. P. White, S. G. Kazarian, K. Hellgardt, M. S. P. Shaffer, C. K. Williams, *Organometallics* **2014**, *33*, 1112; e) D. M. Ermert, I. Ghiviriga, V. J. Catalano, J. Shearer, L. J. Murray, *Angew. Chem. Int. Ed.* **2015**, *54*, 7047; *Angew. Chem.* **2015**, *127*, 7153.
- [28] The FLP P(*t*Bu)₃/ZnEt₂ was also shown to catalyze CO₂ hydrosilylation through initial CO₂ insertion into the Zn–P bond, see: R. Dobrovetsky, D. W. Stephan, *Isr. J. Chem.* **2015**, *55*, 206.
- [29] A compound such as ZnEt₂ may be stored in a sealed tube under a protective CO₂ atmosphere (<https://pubchem.ncbi.nlm.nih.gov/compound/Diethylzinc>). In fact, as early as in 1862 and following the pioneering studies of Franckland on organozinc species, Rieth and Beilstein reported that ZnEt₂ may efficiently be prepared and distilled under CO₂ atmosphere, see: R. Rieth, F. Beilstein, *Liebigs Ann.* **1862**, *123*, 245.
- [30] a) A. Metzger, S. Bernhardt, G. Manolikakes, P. Knochel, *Angew. Chem. Int. Ed.* **2010**, *49*, 4665; *Angew. Chem.* **2010**, *122*, 4769; b) K. Kobayashi, Y. Kondo, *Org. Lett.* **2009**, *11*, 2035. (a) Yeung, C. S.; Dong, V. M. *J. Am. Chem. Soc.* **2008**, *130*, 7826; (b) Ochiai, H.; Jang, M.; Hirano, K.; Yorimitsu, H.; Oshima, K. *Org. Lett.* **2008**, *10*, 2681.
- [31] CO₂ insertion into a Cp–Zn moiety is also known, see: a) S. Schultz, S. Schmidt, D. Bläser, C. Wölper, *Eur. J. Inorg. Chem.* **2011**, 4157; b) P. Jochmann, D. W. Stephan, *Organometallics* **2013**, *32*, 7503.
- [32] For NHC–CO₂ zwitterionic adducts, see: H. A. Duong, T. N. Tekavec, A. M. Arif, J. Louie, *Chem. Commun.* **2004**, 112.
- [33] Though no apparent NHC dissociation is observed for cations 3⁺ and 4⁺ at room temperature, the generation of free NHC (with subsequent formation of the corresponding NHC–CO₂ adduct in the presence of CO₂) cannot be excluded.
- [34] Approximately 10% of the introduced silane HSi(OEt)₃ decomposed over time under catalytic conditions, precluding a quantitative conversion to HCO₂Si(OEt)₃.
- [35] NHCs were reported to hydrosilylate CO₂ in DMF, see: S. N. Riduan, Y. Zhang, J. Y. Ying, *Angew. Chem. Int. Ed.* **2009**, *48*, 3322; *Angew. Chem.* **2009**, *121*, 3372.
- [36] M. M. Deshmukh, S. Sakaki, *Inorg. Chem.* **2014**, *53*, 8485.
- [37] A. J. Arduengo III, H. V. R. Dias, R. L. Harlow, M. Kline, *J. Am. Chem. Soc.* **1992**, *114*, 5530.
- [38] L. Jafarpour, E. D. Stevens, S. P. Nolan, *J. Organomet. Chem.* **2000**, *606*, 49.

Entry for the Table of Contents (Please choose one layout)

Layout 1:

Layout 2:

FULL PAPER



Author(s), Corresponding Author(s)*

Page No. – Page No.

Title